Published in final edited form as:
J Comp Neurol. 2022 February ; 530(3): 648–655. doi:10.1002/cne.25236.

A sex-specific feedback projection from aromatase-expressing neurons in the medial amygdala to the accessory olfactory bulb

Tal Inbar[‡], **Rachel Davis**[*], **Joseph F. Bergan**[*,‡]

[‡]Neuroscience and Behavior Graduate Program, University of Massachusetts at Amherst

[*]Department of Psychological and Brain Sciences, University of Massachusetts at Amherst

Abstract

The accessory olfactory bulb (AOB) plays a critical role in classifying pheromonal signals. Here we identify two previously undescribed sources of aromatase signaling in the AOB: 1) A population of aromatase-expressing neurons in the AOB itself; 2) A tract of aromatase-expressing axons which originate in the ventral medial amygdala (MEA) and terminate in the AOB. Using a retrograde tracer in conjunction with a transgenic strategy to label aromatase-expressing neurons throughout the brain, we found that a single contiguous population of neurons in the ventral MEA provides the only significant feedback by aromatase-expressing neurons to the AOB. This population expresses the estrogen receptor alpha (ERα) and displayed anatomical sex-differences in the number of neurons (higher in male mice) and the size of cell bodies (larger in females). Given the previously established relationship between aromatase-expression, estrogen signaling, and the function of sexually dimorphic circuits, we suggest that this feed-back population is well-positioned to provide neuroendocrine feedback to modulate sensory processing of social stimuli in the AOB.

Graphical Abstract

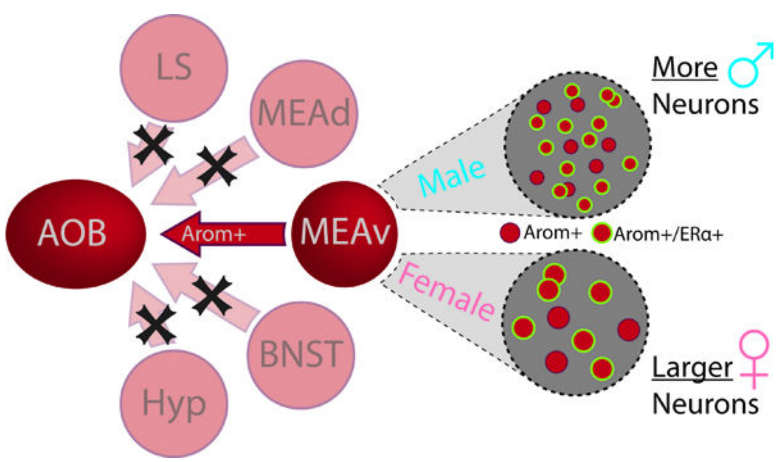

AUTHOR CONTRIBUTIONS: T.I. and J.F.B. conceived and designed all experiments. T.I., J.F.B. and R.D. collected the data. J.F.B. and T.I. analyzed the data and wrote the manuscript with help from R.D.:

CONFLICT OF INTEREST: The authors declare no conflict of interest.

Aromatase neurons are distributed in clustered populations primarily in a network of brain regions (red) devoted to social behavior. Out of all potential sources of aromatase neurons, only the ventral medial amygdala projects back to the accessory olfactory bulb. The population of aromatase-expressing neurons in the ventral medial amygdala also expresses Erα and displays two sex differences: 1) aromatase-expressing neurons are larger in females; 2) there are more aromatase-expressing neurons in male mice.

Keywords

Aromatase; Medial Amygdala; Olfactory; Vomeronasal; Pheromones; Feedback

INTRODUCTION:

Sensory perception relies on both feed forward and feedback connections within sensory circuits. Feedback projections can modulate the representation of sensory cues as early as the sensory epithelium (Repérant et al., 2007; Cherian et al., 2014; Keesom and Hurley, 2020), including in chemosensory circuits (Broadwell and Jacobowitz 1976; Chae et al., 2018). Mice rely heavily on the detection of specific chemicals by the vomeronasal organ to identify and respond to potential social partners (Dulac and Wagner, 2006; Liberles, 2014). Therefore, pinpointing the sources of feedback and modulation of early sensory representations is an important aspect of understanding how the brain produces social behavior in mice.

Chemical cues are detected by multiple complementary sensory systems in mice: the main olfactory system, which detects volatile odorants, and the vomeronasal system which detects non-volatile chemosignals (Powers and Winans, 1975; Dulac and Torello, 2003; Halpern and Martinez-Marcos, 2003; Kimchi et al., 2007). Impairments to the vomeronasal system disrupt innate behaviors such as reproduction, territorial aggression, parenting, and predatory avoidance (Stowers et al., 2002; Keller et al., 2006; Kimchi et al., 2007; Hasen and Gammie, 2009; Isogai et al., 2011). Sensory neurons in the vomeronasal organ synapse in the AOB which, in-turn, broadcasts this information to an evolutionarily conserved Social Behavior Network in the basal forebrain within the basal forebrain, hypothalamus, and midbrain (SBN; Newman, 1999) that controls social behavior and neuroendocrine responses. The social behaviors elicited by a specific stimulus can vary depending on the age, sex, neuroendocrine state, and the past experiences of each animal. Within the SBN, feedback from the MEA to the AOB plays an important role in modulating the behavioral response to social stimuli based on an animal’s internal state (Newman, 1999; Fan and Luo, 2009).

In this study, we characterize aromatase expression in the AOB. Aromatase is the enzyme responsible for converting testosterone into estradiol. Specifically, we define two populations of aromatase-expressing neurons that interact with the AOB—one within the AOB itself and a tract of aromatase-expressing axons that originate from neurons in the ventral MEA and terminate in the AOB. To our knowledge, neither population has been previously identified. Although several aromatase-expressing (arom+) populations of neurons are distributed throughout the brain, the vast majority of arom+ neurons reside in the SBN. The largest population of arom+ neurons in the mouse brain is in the MEA, and these neurons have been implicated in the control of territorial aggression, social investigation, and social memory (Ferguson et al., 2001; Unger et al., 2015; Yao et al., 2017). Arom+ MEA neurons mediate behaviors with clear sex-differences and, correspondingly, sex-differences have been identified for both the afferent and efferent synaptic connections of these neurons (Wu et al., 2009; Billing et al., 2020). Thus, arom+ MEA neurons represent a central node in the SBN that can integrate sensory information with neuroendocrine status to generate social behaviors.

Here, we use a transgenic approach to label arom+ neurons throughout the brain in conjunction with retrograde tracing to identify the source of arom+ feedback to the AOB. This approach identified a small subset of arom+ neurons in the MEA. In contrast to the large population of arom+ neurons located in the posterodorsal MEA (MEApd), the population described here is located along the ventral surface of the MEA (MEAv) and extends across the full anterior to posterior extent of the ventral MEA. This finding demonstrates that there are at least two distinct populations of arom+ neurons in the MEA, which are anatomically separated and maintain different connectivity with the AOB. Given the role of aromatase in establishing sexually dimorphic circuits, and in accord with the role of estradiol in modulating vomeronasal responses (Cherian et al., 2014), we hypothesize that this feed-back population is well-positioned to integrate sensory and neuroendocrine information and, ultimately, modulate the representation of social stimuli in the AOB.

METHODS:

Animals:

All mice (*mus musculus*) used in this study were housed and maintained on a 12-hour light-dark cycle with 24-hour access to food and water available ad libitum. Animals remained group-housed in single-sex cages prior to surgery, after which they were placed in single-housing for recovery. All animal care and experiments were carried out in accordance with NIH guidelines and protocols approved by the Institutional Animal Care and Use Committee at the University of Massachusetts in Amherst (IACUC; protocol #2018–0014 and #2017–0060). Euthanasia of mice was performed using isoflurane (2–5%) to induce deep anesthesia followed by cervical dislocation.

The aromatase expression was identified using a double-transgenic mouse line generated by cross-breeding a homozygous aromatase-cre mouse with a homozygous Rosa26-lsl-tdTomato reporter. The aromatase-cre transgenic line was reported previously and displays faithful expression (Yao et al., 2017). The Rosa26-lsl-tdTomato reporter line (Ai9) was purchased from Jackson Labs (Maine; Madisen et al., 2010). Arom+ neurons could then be observed with fluorescent microscopy images acquired using a Zeiss Apotome with an AxioCam digital camera and AxioVision software (Zeiss; NY).

Fluorogold Injections:

Fluorogold (Fluorochrome Inc., Englewood CO) was dissolved in deionized distilled water to make a 2% solution. Animals were anesthetized with isoflurane throughout the stereotaxic injection. A small cut was made over the AOB and a craniotomy was performed over the olfactory bulbs, rostral to, but as close as possible to the rhinal sinus prior to fluorogold injection (Ben-Shaul et al., 2010). Each animal received 5 bilateral pressure injections (100 nL each) starting at the ventral surface of the AOB, serially ascending 250μm at a 45-degree angle, using a hydraulic microinjector and 20μm glass capillary. Each injection volume was delivered over 2 minutes with a 5-minute rest period after each injection and before the pipette was moved to the next site. Animals were maintained 10 days after the stereotaxic injection to allow retrograde transport of fluorogold from axons in the AOB to cell bodies in the brain.

Tissue Preparation and Histology:

Animals were anesthetized and transcardially perfused with phosphate buffer solution followed by 4% paraformaldehyde in phosphate buffer solution. Perfused brains were post-fixed in 4% paraformaldehyde for 1 day prior to being sectioned coronally at 100μm with a vibratome. Olfactory bulbs were sectioned on the parasagittal plane at 100 μm thickness. A subset of tissue sections was counter-stained for cell nuclei with TOPRO-3 prior to mounting on slides. Immunohistochemistry was performed on tissue sections as described above. Sections were bathed in 10% FBS in 0.5% TritonX-100/PBS blocking solution for one hour at room temperature. Sections were then incubated overnight at 4°C in rabbit polyclonal anti-ERα primary antibody (06–935, 1:1000; Millipore Sigma). Sections were then washed 3 times in 0.05% tritonX-100 in PBS (5 minutes; 20 minutes; 40 minutes) and incubated with an Alexa Fluor 488-conjugated goat anti-rabbit IgG (1:200; Jackson ImmunoResearch). Sections were then washed 3 times in 0.05% tritonX-100 in PBS (5 minutes; 20 minutes; 40 minutes) and mounted on slides for fluorescence microscopy. Analyses investigating the expression of ERα and sex differences in the number of arom+ neurons considered the entire contiguous population of arom+ neurons in the ventral MEA.

Data Analysis:

All the analyses adhered to the ARRIVE guidelines. To generate cell counts, a trained blind observer was presented with images and cell locations were recorded using custom MATLAB (Mathworks, MA) scripts. The borders of brain regions were outlined by a trained observer, blind to the fluorogold signal, based on the Paxinos atlas (Franklin and Paxinos, 2008). Statistical analyses and figure generation were performed using validated MATLAB scripts. Comparisons between two groups were performed with an unpaired t-test. To measure soma sizes, cropped images were made centered on all counted neurons and a randomized sample were presented to a trained blind observer to measure the long and short axes of the soma. Areas were then estimated by calculating their corresponding ellipsis which was compared between males and females using a 2-way nested ANOVA. Statistical results were considered significant at $p < 0.05$ with Bonferroni correction to identify significant differences when considering multiple comparisons. Cohen's d was calculated by finding the difference of means between each group and dividing by the pooled SD. All means are reported with SEM measurements.

RESULTS:

The aromatase-cre line crossed with the Ai9 tdTomato reporter line brightly labeled aromatase-expressing (arom+) neurons (Yao, et al. 2017), and we examined brain-wide expression in regions with previously established aromatase expression to confirm the veracity of the reporter line. Arom+ neurons were found in the lateral septum, ventral pallidum, medial amygdala, bed nucleus of the stria terminalis, posterior cortical amygdala, hypothalamus, and sparsely in the hippocampus (Figure 1A). This distribution is consistent with previous reports of the expression of aromatase in the mouse brain (MacLusky et al., 1987; Balthazart et al., 1990; Balthazart et al. 1991; Wagner and Morrell, 1997; Yao et al., 2018;).

A previously undescribed arom+ fiber bundle was observed in the AOB with a small population of arom+ neurons intercalated within this fiber tract. All cell bodies and fibers for aromatase neurons in the olfactory bulb were specific to the AOB and not present in the MOB (Figure 1B). All identified arom+ cell bodies in the olfactory bulb were in the AOB (9 animals; 204 neurons) and no arom+ neurons were identified in the MOB indicating that the distribution of arom+ neurons in the olfactory bulb is highly selective for the AOB ($p=0.0004$, two-sample t-test). Closer examination of arom+ neurons in the AOB revealed neurons in the mitral cell layer (10.8 ± 2.3%), granule cell layer (22.8 ± 4.5%), and dorsolateral olfactory tract (66.5 ± 4.2%; Figure 1C).

To determine the source of arom+ fibers in the AOB, we injected fluorogold in the AOB of aromatase reporter mice to retrogradely label the cell bodies of neurons that project to the AOB (arom+→AOB; Figure 2A, B). No significant co-labeling of arom+ neurons with fluorogold was observed in most arom+ populations (Figure 2C, D). The thalamus (TH; arom+→AOB = 0.06 ± 0.5 SEM % of total) and posteromedial cortical amygdala (PMCo; arom+→AOB = 0.07 ± 0.06 SEM % of total) contained mutually exclusive populations of fluorogold labeled neurons and Arom+ neurons that were interwoven but non-overlapping. The piriform cortex (Pir; arom+→AOB = 0.85 ± 0.43 SEM % of total) and posterodorsal subnucleus of the media amygdala contained some co-labeled neurons but these represent a small fraction of the total arom+ population (MEApd; arom+→AOB = 0.33 ± 0.11 SEM % of total). Thus, while each of the above areas contains a robust population of arom+ neurons and/or feedback projections to the AOB, none of these populations contributes significantly to the arom+→AOB population (Figure 2D; $p>0.2$; single sample t-test with Bonferroni correction).

A single contiguous population of arom+ neurons in the ventral MEA (MEAv) was retrogradely labeled from fluorogold microinjections in the AOB (Figure 3A). The vast majority of MEAv arom+ neurons synapse on the AOB (Figure 3B) with at least 84.7 ± 4.5 SEM percent of arom+ MEAv neurons co-labeled for fluorogold ($p<0.00001$, single sample t-test; 50.8 ± 9.7 SEM average MEAv col-labeled neurons per slice). The population of arom+ neurons in the ventral MeA constitutes 97.5 ± 0.9 SEM percent of all arom+→AOB projecting neurons in the brain (Figure 3C; $p<0.00001$, two sample t-test) and is anatomically distinct from a much larger population of arom+ neurons in the MEApd (Figure 3D). Thus, in addition to their cell bodies being anatomically separated from the larger population of aromatase neurons in the MEApd, arom+ in MEAv are the only population of arom+ neurons that synapse on the AOB. The ventral population of arom+→AOB neurons spanned the anterior-posterior axis of the MeA and the fraction of arom+→AOB neurons was similar across the anterior to posterior axis suggesting that, at least in terms of connectivity with the AOB, this is a homogenous population.

Because aromatase neurons produce estradiol, we immunostained for estrogen receptor alpha (ERα) in aromatase reporter animals. Most neurons contiguous with the arom+→AOB population expressed both ERα and tdTomato (59.0 ± 2.8 % SEM), while smaller fractions expressed only tdTomato (14.2 ± 2.3 % SEM) or ERα (26.8 ± 3.2 % SEM). Therefore, roughly 80 percent of the MEAv arom+ population that projects back to the AOB also express ERα (Figure 4 A, B), and the fraction of MEAv neurons that co-labeled for aromatase and ERα was similar in males and females ($p = 0.67$, two-sample t-test). However, the population of arom+ neurons in the ventral MeA contains more neurons in male versus female animals (Figure 4C; male: 44.28 ± 6.76 SEM average neurons/slice; female: 27.78 ± 2.84 SEM average neurons/slice; $p=0.039$, two-sample t-test), while the soma area of these neurons were modestly smaller in males versus females (figure 4D; males: 301.7 ± 3.7 μm^2 SEM; female: 330 ± 3.0 μm^2 SEM; $p = 0.0042$, two-way nested ANOVA).

DISCUSSION:

Here, we report a small population of arom+ neurons that are specific to the AOB and show that the AOB is dense with aromatase-positive fibers originating from a contiguous population of neurons located in the ventral MeA. Consistent with previous findings, these fibers terminated most densely in the granule cell layer of the AOB (Fan and Luo., 2009; Oboti et al., 2018). Feedback to early sensory regions is a common and critical feature of circuit organization. The feedback population described here is unique in that: 1) Seemingly all arom+ neurons in this population project back to the AOB; 2) It originates from a single small and contiguous population of arom+ neurons in the ventral MeA; 3) It is the first report of distinct sub-populations of arom+ neurons within the MeA; 4) It specifically targets the AOB and not the MOB. This degree of feedback specificity (a single population of arom+ neurons accounts for nearly all feedback to the AOB) implies that the population of arom+ neurons described here are quite restricted and, therefore, may provide specific contributions to the processing of pheromones and production of social behavior.

The mutual dissociation of cell body location and synaptic connectivity to the AOB definitively demonstrate at least two distinct subpopulations of arom+ neurons in the MeA: 1) a large subpopulation of arom+ neurons in the posterodorsal MeA that is implicated in aggression and the modulation of social investigation by oxytocin (Unger et al., 2015; Yao et al., 2017) that does not send afferent fibers to the AOB; 2) a smaller subpopulation of arom+ neurons in the ventral MeA that project directly to the AOB, described here, whose function remains uncharacterized. These results highlight the heterogeneity of aromatase neurons in the MEA, which is likely to extend well beyond the two subpopulations outlined here.

Roughly 98% of arom+→AOB neurons are part of a single population of neurons spanning the ventral MeA. The remaining 2% were distributed over several brain regions with none of these populations reaching statistical significance. The specificity of this finding provides insight regarding the potential functions of arom+ feedback to the AOB. First, the AOB and ventral MEA are both integral nodes in the vomeronasal pathway that mediates detection of pheromones, detection of allomones, and the regulation of social behaviors (Fernandez-Fewell and Meredith, 1994; Samuelsen and Meredith, 2009; Choi et al.,2005; Ben-Shaul et al., 2010; Bergan et al., 2014). For example, electrolytic lesions of the homologous region induced changes in parental behavior in both male and female rats (Del Cerro et al., 1991; Izquierdo et al., 1992). Neural activity in the MEApv is involved in mate selection, territorial aggression, and the detection of predator odors (Choi et al.,2005; Ishii et al., 2017), and neurons projecting from the MEA to the AOB are known to convey opposite-sex stimuli (Martel and Baum, 2009). Moreover, estrogens modulate social behavior and enhance an animal's ability to discriminate social odors directly at the olfactory bulb (Woodley & Baum, 2004). Given the extensive literature linking the MeA and AOB to social behavior, in accord with the role of aromatase in establishing sex-specific social behaviors and the role of estrogens in modulating chemosensory responses, we hypothesize that the arom+→AOB population may shape sensory processing of social stimuli in the AOB.

Aromatase acts during development as well as on a moment-to-moment basis in adults to produce estradiol which can modify the function of neural circuits. Aromatase is implicated in establishing anatomical and functional sex-differences in the brain (Bakker et al., 2002; Morris et al., 2004; McCarthy, 2008; Bergan et al., 2014, Yao et al., 2017), and both anatomical and functional sex-differences have previously been established in the AOB (Valencia et al., 1986; Halem et al., 2001). One possibility is that aromatase is involved in organizing sex difference locally in the AOB or through the arom+ feedback projection to the AOB during development. Consistent with previous reports on sex differences in the MEAv (Collado et al., 1990) and more broadly of populations of arom+ neurons in the brain, MEAv arom+ neurons display a clear sex-difference in cell quantities.

Aromatase and estradiol are also involved in short-term regulation of behavior in adulthood (Balthazart and Ball, 2006; Remage-Healey and Bass, 2006) and in modulating the activity of vomeronasal sensory neurons directly (Cherian et al., 2014). The ventral MEA arom+→AOB population described here expresses ERα and therefore may have the capacity to respond to changes in circulating levels of estradiol such as the estrus cycle, pregnancy, or postpartum period by altering either their electrical activity or gene expression profile. Another intriguing possibility is that this population may secrete estradiol either locally in a paracrine fashion or at their axonal terminals in a synaptocrine fashion in the AOB (see Saldanha et al., 2011). While we focused on estrogen receptors, our data cannot rule out the possibility that aromatase could also act as an androgen sink in this population. In agreement with previous reports in the hypothalamus (Moffitt et al., 2018), we found that aromatase and ERα colocalized in individual neurons; however, we also identified neurons that expressed only aromatase or ERα in the MEAv, potentially indicating both autocrine and paracrine roles for estradiol within the MEAv.

Given that the AOB is a mandatory node in the vomeronasal processing of pheromones, modulation of AOB function is likely to propagate to virtually all other nodes of the SBN (Figure 5; Kevetter and Winans, 1981). Given the need to adapt social behavior to an animal's sex, age, endocrine state, and past experiences, understanding how the brain modulates early pheromonal processing in the AOB is an important goal. This anatomical observation provides a clear target for future investigations into the role of arom+→AOB neurons in the ventral MEA for modifying chemosensory processing of social cues in the AOB and, ultimately, the production of social behavior.

ACKNOWLEDGMENTS:

We thank Luke Remage-Healey and Diane Kelly for helpful comments on earlier versions of this paper. Support for these experiments came from the University of Massachusetts at Amherst and the National Institutes of Health R01MH115094–01A1 (J.F.B)

DATA AVAILABILITY STATEMENT:

All data and analysis scripts have been made available.

REFERENCES:

Bakker J, Honda S, Harada N, & Balthazart J. (2002). Sexual partner preference requires a functional aromatase (cyp19) gene in male mice. Hormones and behavior, 42(2), 158–171. [PubMed: 12367569]

Balthazart J, & Ball GF (2006). Is brain estradiol a hormone or a neurotransmitter? Trends in neurosciences, 29(5), 241–249. [PubMed: 16580076]

Balthazart J, Foidart A, Surlemont C, & Harada N. (1991). Distribution of aromatase-immunoreactive cells in the mouse forebrain. Cell and tissue research, 263(1), 71–79. [PubMed: 2009554]

Balthazart J, Foidart A, Surlemont C, Vockel A, & Harada N. (1990). Distribution of aromatase in the brain of the Japanese quail, ring dove, and zebra finch: an immunocytochemical study. Journal of comparative neurology, 301(2), 276–288.

Ben-Shaul Y, Katz LC, Mooney R, & Dulac C. (2010). In vivo vomeronasal stimulation reveals sensory encoding of conspecific and allospecific cues by the mouse accessory olfactory bulb. Proceedings of the National Academy of Sciences, 107(11), 5172–5177.

Bergan JF, Ben-Shaul Y, & Dulac C. (2014). Sex-specific processing of social cues in the medial amygdala. Elife, 3, e02743. [PubMed: 24894465]

Billing A, Correia MH, Kelly DA, Li GL, & Bergan JF (2020). Synaptic connections of aromatase circuits in the medial amygdala are sex specific. Eneuro, 7(3).

Broadwell RD, & Jacobowitz DM (1976). Olfactory relationships of the telencephalon and diencephalon in the rabbit. III. The ipsilateral centrifugal fibers to the olfactory bulbar and retrobulbar formations. Journal of Comparative Neurology, 170(3), 321–345.

Chae H, Otazu GH, & Albeanu DF (2018). Anterior olfactory nucleus and piriform cortex feedback differentially modulate olfactory bulb output neurons. Chemical Senses, 43(4), E74–E75.

Cherian S, Lam YW, McDaniels I, Struziak M, & Delay RJ (2014). Estradiol rapidly modulates odor responses in mouse vomeronasal sensory neurons. Neuroscience, 269, 43–58. [PubMed: 24680884]

Choi GB, Dong HW, Murphy AJ, Valenzuela DM, Yancopoulos GD, Swanson LW, & Anderson DJ (2005). Lhx6 delineates a pathway mediating innate reproductive behaviors from the amygdala to the hypothalamus. Neuron, 46(4), 647–660. [PubMed: 15944132]

Collado P, Guillamón A, Valencia A, & Segovia S. (1990). Sexual dimorphism in the bed nucleus of the accessory olfactory tract in the rat. Developmental Brain Research, 56(2), 263–268. [PubMed: 2261686]

Del Cerro MCR, Izquierdo MAP, Collado P, Segovia S, & Guillamón A. (1991). Bilateral lesions of the bed nucleus of the accessory olfactory tract facilitate maternal behavior in virgin female rats. Physiology & behavior, 50(1), 67–71. [PubMed: 1946733]

Dulac C, & Torello AT (2003). Molecular detection of pheromone signals in mammals: from genes to behaviour. Nature Reviews Neuroscience, 4(7), 551–562. [PubMed: 12838330]

Dulac C, & Wagner S. (2006). Genetic analysis of brain circuits underlying pheromone signaling. Annu. Rev. Genet, 40, 449–467. [PubMed: 16953793]

Fan S, & Luo M. (2009). The organization of feedback projections in a pathway important for processing pheromonal signals. Neuroscience, 161(2), 489–500. [PubMed: 19341782]

Ferguson JN, Aldag JM, Insel TR, & Young LJ (2001). Oxytocin in the medial amygdala is essential for social recognition in the mouse. Journal of Neuroscience, 21(20), 8278–8285. [PubMed: 11588199]

Fernandez-Fewell GD, & Meredith M. (1994). C-fos expression in vomeronasal pathways of mated or pheromone-stimulated male golden hamsters: contributions from vomeronasal sensory input and expression related to mating performance. Journal of Neuroscience, 14(6), 3643–3654. [PubMed: 8207479]

Halem HA, Baum MJ, & Cherry JA (2001). Sex difference and steroid modulation of pheromone-induced immediate early genes in the two zones of the mouse accessory olfactory system. Journal of Neuroscience, 21(7), 2474–2480. [PubMed: 11264321]

Hasen NS, & Gammie SC (2009). Trpc2 gene impacts on maternal aggression, accessory olfactory bulb anatomy and brain activity. Genes, Brain and Behavior, 8(7), 639–649.

Ishii KK, Osakada T, Mori H, Miyasaka N, Yoshihara Y, Miyamichi K, & Touhara K. (2017). A labeled-line neural circuit for pheromone-mediated sexual behaviors in mice. Neuron, 95(1), 123–137. [PubMed: 28648498]

Isogai Y, Si S, Pont-Lezica L, Tan T, Kapoor V, Murthy VN, & Dulac C. (2011). Molecular organization of vomeronasal chemoreception. Nature, 478(7368), 241–245. [PubMed: 21937988]

Izquierdo MAP, Collado P, Segovia S, Guillamón A, & Del Cerro MCR (1992). Maternal behavior induced in male rats by bilateral lesions of the bed nucleus of the accessory olfactory tract. Physiology & behavior, 52(4), 707–712. [PubMed: 1409941]

Keesom SM, & Hurley LM (2020). Silence, Solitude, and Serotonin: Neural Mechanisms Linking Hearing Loss and Social Isolation. Brain sciences, 10(6), 367.

Keller M, Pierman S, Douhard Q, Baum MJ, & Bakker J. (2006). The vomeronasal organ is required for the expression of lordosis behaviour, but not sex discrimination in female mice. European Journal of Neuroscience, 23(2), 521–530.

Kevetter GA, & Winans SS (1981). Connections of the corticomedial amygdala in the golden hamster. I. Efferents of the "vomeronasal amygdala". Journal of Comparative Neurology, 197(1), 81–98.

Kimchi T, Xu J, & Dulac C. (2007). A functional circuit underlying male sexual behaviour in the female mouse brain. Nature, 448(7157), 1009–1014. [PubMed: 17676034]

Liberles SD (2014). Mammalian pheromones. Annual review of physiology, 76, 151–175.

MacLusky NJ, Clark AS, Naftolin F, & Goldman-Rakic PS (1987). Estrogen formation in the mammalian brain: possible role of aromatase in sexual differentiation of the hippocampus and neocortex. Steroids, 50(4–6), 459–474. [PubMed: 3332936]

Madisen L, Zwingman TA, Sunkin SM, Oh SW, Zariwala HA, Gu H, Ng LL, Palmiter R, et al. , (2010). A robust and high-throughput Cre reporting and characterization system for the whole mouse brain. Nature neuroscience, 13(1), 133. [PubMed: 20023653]

Martel KL, Baum MJ. (2009). A centrifugal pathway to the mouse accessory olfactory bulb from the medial amygdala conveys gender-specific volatile pheromonal signals. Eur J Neurosci. 29(2):368–76. [PubMed: 19077123]

Morris JA, Jordan CL, & Breedlove SM (2004). Sexual differentiation of the vertebrate nervous system. Nature neuroscience, 7(10), 1034–1039. [PubMed: 15452574]

Halpern M, & Martınez-Marcos A. (2003). Structure and function of the vomeronasal system: an update. Progress in neurobiology, 70(3), 245–318. [PubMed: 12951145]

McCarthy MM (2008). Estradiol and the developing brain. Physiological reviews, 88(1), 91–134. [PubMed: 18195084]

Moffitt JR, Bambah-Mukku D, Eichhorn SW, Vaughn E, Shekhar K, Perez JD, Rubenstein ND, Junjie H, Regev A, Dulac C, Zhuang X. (2018). Molecular, spatial, and functional single-cell profiling of the hypothalamic preoptic region. Science, 362(6416).

Newman SW (1999). The medial extended amygdala in male reproductive behavior a node in the mammalian social behavior network. Annals of the New York Academy of Sciences, 877(1), 242–257. [PubMed: 10415653]

Oboti L, Russo E, Tran T, Durstewitz D, & Corbin JG (2018). Amygdala corticofugal input shapes mitral cell responses in the accessory olfactory bulb. Eneuro, 5(3).

Paxinos G, & Franklin KB (2019). Paxinos and Franklin's the mouse brain in stereotaxic coordinates. Academic press.

Powers JB, & Winans SS (1975). Vomeronasal organ: critical role in mediating sexual behavior of the male hamster. Science, 187(4180), 961–963. [PubMed: 1145182]

Remage-Healey L, & Bass AH (2006). A rapid neuromodulatory role for steroid hormones in the control of reproductive behavior. Brain research, 1126(1), 27–35. [PubMed: 16854385]

Repérant J, Médina M, Ward R, Miceli D, Kenigfest NB, Rio JP, & Vesselkin NP (2007). The evolution of the centrifugal visual system of vertebrates. A cladistic analysis and new hypotheses. Brain Research Reviews, 53(1), 161–197. [PubMed: 17059846]

Saldanha CJ, Remage-Healey L, Schlinger BA. (2011). Synaptocrine signaling: steroid synthesis and action at the synapse. Endocr Rev. 2011 32(4):532–49. [PubMed: 21622487]

Samuelsen CL, Meredith M. (2009). The vomeronasal organ is required for the male mouse medial amygdala response to chemical-communication signals, as assessed by immediate early gene expression. Neuroscience. 2164(4):1468–76.

Stowers L, Holy TE, Meister M, Dulac C, & Koentges G. (2002). Loss of sex discrimination and male-male aggression in mice deficient for TRP2. Science, 295(5559), 1493–1500. [PubMed: 11823606]

Unger EK, Burke KJ Jr, Yang CF, Bender KJ, Fuller PM, & Shah NM (2015). Medial amygdalar aromatase neurons regulate aggression in both sexes. Cell reports, 10(4), 453–462. [PubMed: 25620703]

Valencia A, Segovia S, & Guillamón A. (1986). Effects of sex steroids on the development of the accessory olfactory bulb mitral cells in the rat. Developmental Brain Research, 24(1–2), 287–290.

Wagner CK, & Morrell JI (1997). Neuroanatomical distribution of aromatase mRNA in the rat brain: indications of regional regulation. The Journal of steroid biochemistry and molecular biology, 61(3–6), 307–314. [PubMed: 9365206]

Wang Q, Ding SL, Li Y, Royall J, Feng D, Lesnar P, Graddis N, Naeemi M, et al. (2020). The Allen mouse brain common coordinate framework: a 3D reference atlas. Cell, 181(4), 936–953. [PubMed: 32386544]

Wu MV, Manoli DS, Fraser EJ, Coats JK, Tollkuhn J, Honda SI, Harada N, & Shah NM (2009). Estrogen masculinizes neural pathways and sex-specific behaviors. Cell, 139(1), 61–72. [PubMed: 19804754]

Yao S, Bergan J, Lanjuin A, & Dulac C. (2017). Oxytocin signaling in the medial amygdala is required for sex discrimination of social cues. Elife, 6, e31373. [PubMed: 29231812]

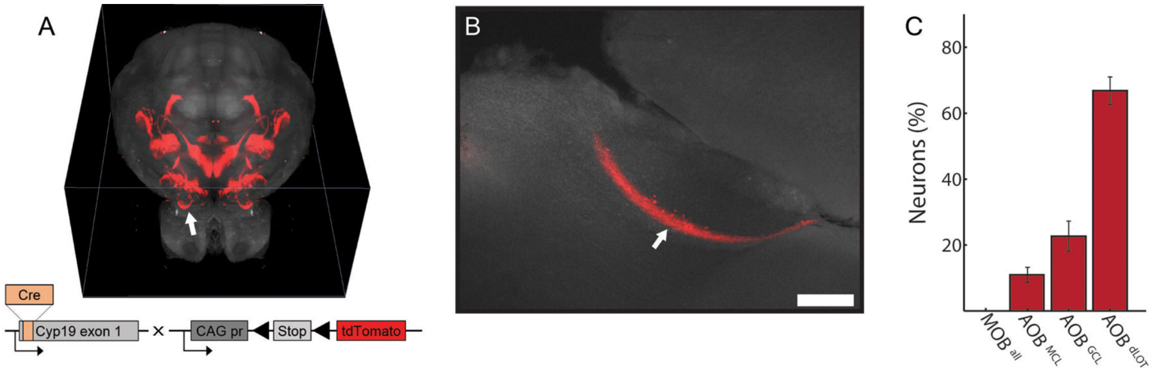

Figure 1.

Aromatase expression in the accessory olfactory bulb. A, Whole brain distribution of arom+ neurons (red) was visualized by crossing a transgenic mouse line expressing Cre in arom+ neurons with a tdTomato reporter line (grey: autofluorescence for contrast). B, Arom+ fibers and cell bodies were visualized in the AOB and not in the MOB. C, Arom+ neurons were sparsely located in the dorsolateral olfactory tract (AOB^{dLOT}), granule cell layer (AOB^{GCL}), and mitral cell layer (AOB^{MCL}). Arrows indicate the arom+ fiber, with intercalated arom+ cells, in the AOB.

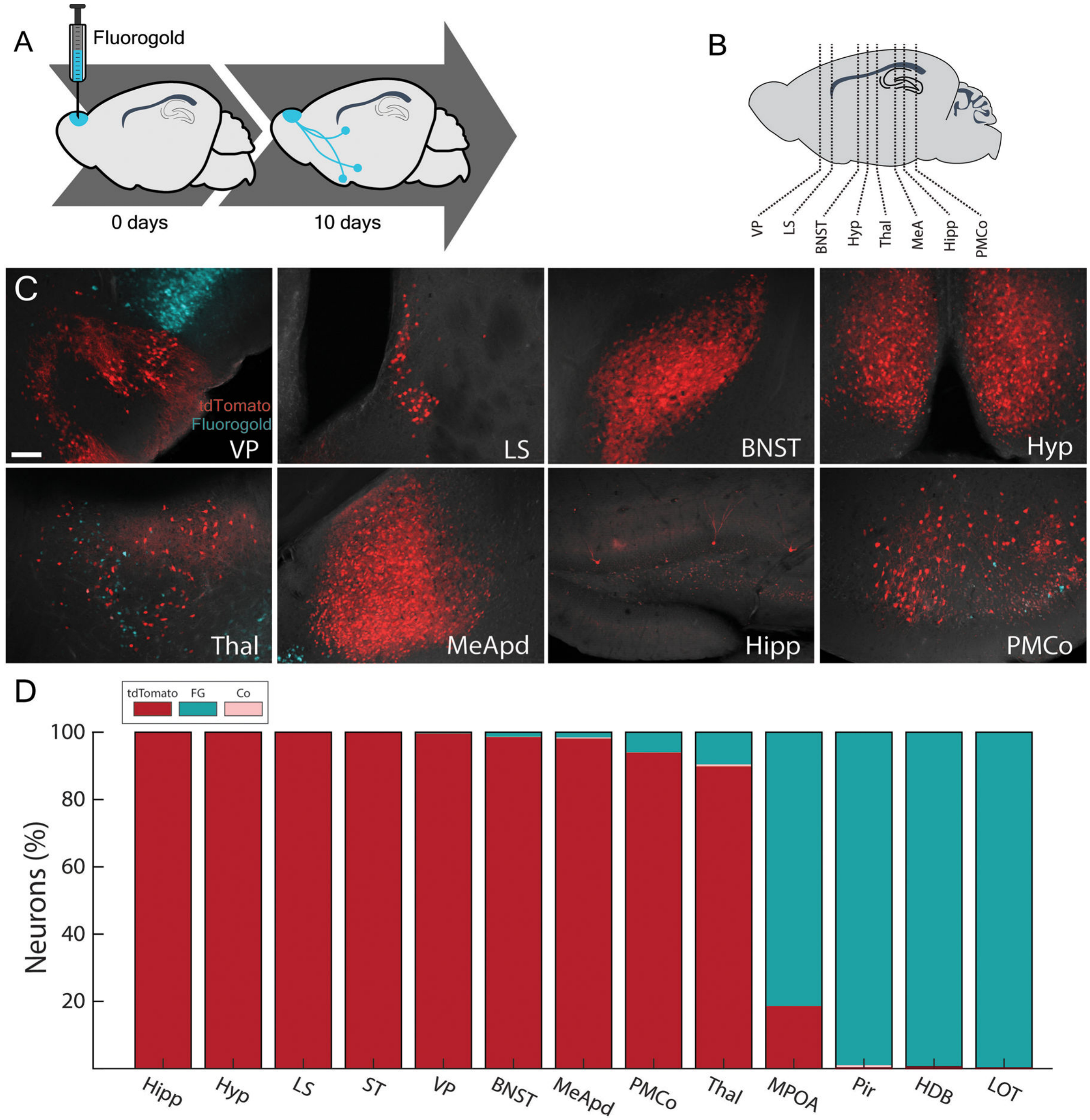

Figure 2.

Most arom+ neuron populations in the brain do not project back to the AOB. A, Fluorogold (cyan) was microinjected in the AOB of arom+ reporter mice to retrogradely label AOB projecting neurons in the brain. B, Slices from major populations of arom+ neurons spanning the anterior to posterior axis of the brain were analyzed. C, Injections of fluorogold in the AOB retrogradely labeled AOB projecting neurons (cyan) near, but not including, arom+ populations (red) in the brain. D, Thirteen brain regions were identified that had either large populations of arom+ neurons (red) or large populations of AOB projecting neurons (cyan); however, most regions lacked statistically significant co-labeling of fluorogold with arom+ (pink; $P > 0.5$; one-sample t-test with Bonferroni correction). Abbreviations: hippocampus (Hipp), hypothalamus (Hyp), lateral septum (LS), Striatum (ST), ventral pallidum (VP), bed nucleus of the stria terminalis (BNST), posterodorsal

Author Manuscript

Author Manuscript

Author Manuscript

medial amygdala (MEApd), or posteromedial amygdala (PMCO). thalamus (Th), medial preoptic area (MPOA), piriform cortex (Pir), Horizontal Diagonal Band (HDB), lateral olfactory tract (LOT).

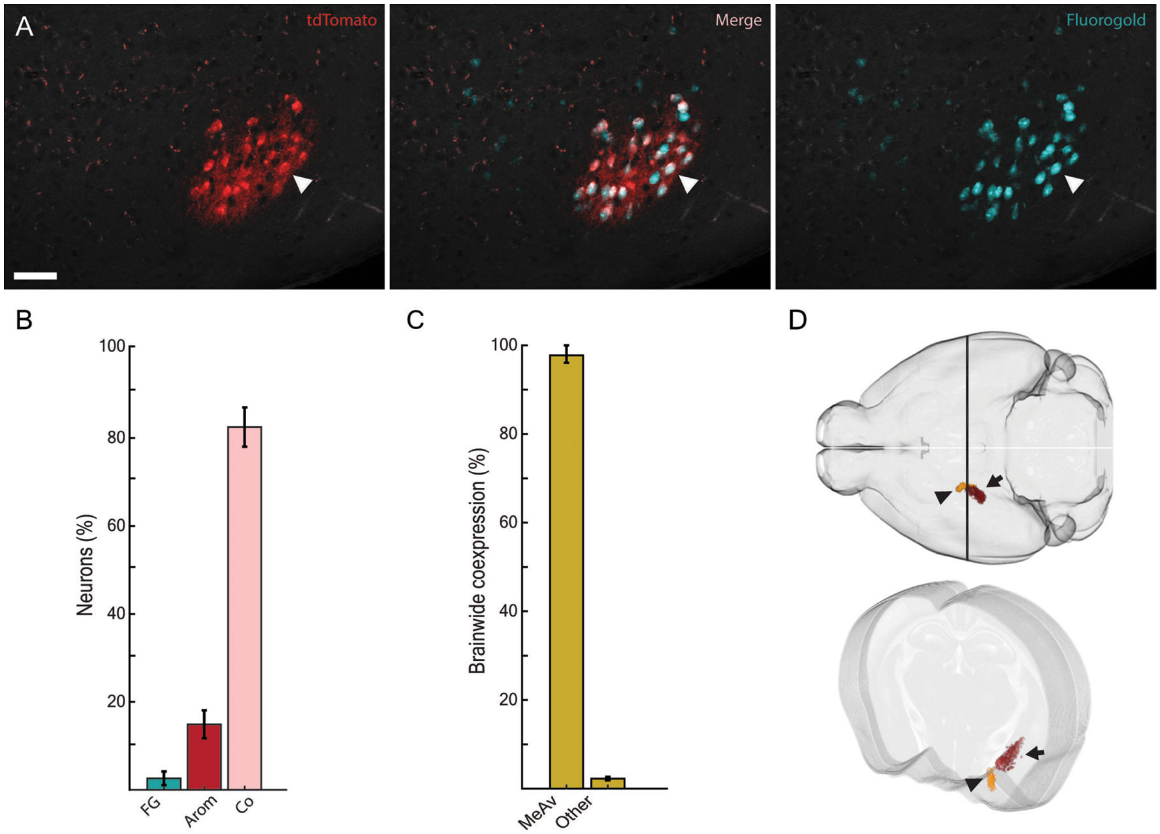

Figure 3.

Arom+ neurons in the ventral MEA project to the AOB. A, Aromatase (red) and fluorogold from an AOB injection (cyan) strongly colocalize in the MEAv (arrowhead: co-labeled neuron). B, Most arom+ MEAv neurons project to the AOB and are co-labeled by fluorogold ($p<0.00001$, single sample t-test). C, The small population of arom+ neurons in the MEAv constitutes approximately 98% of all arom+→AOB neurons in the brain excluding the arom+ AOB population. D, A 3D rendering of arom+ neurons in the MeA is shown registered to the Allen Institute reference mouse brain (Allen Institute for Brain Science, 2004, Wang et al., 2020). Neurons that were labeled by fluorogold (orange; arrowhead) project to the AOB and are more anterior and ventral than the population of arom+ neurons in the MEApd (red; arrow) that do not project back to the AOB.

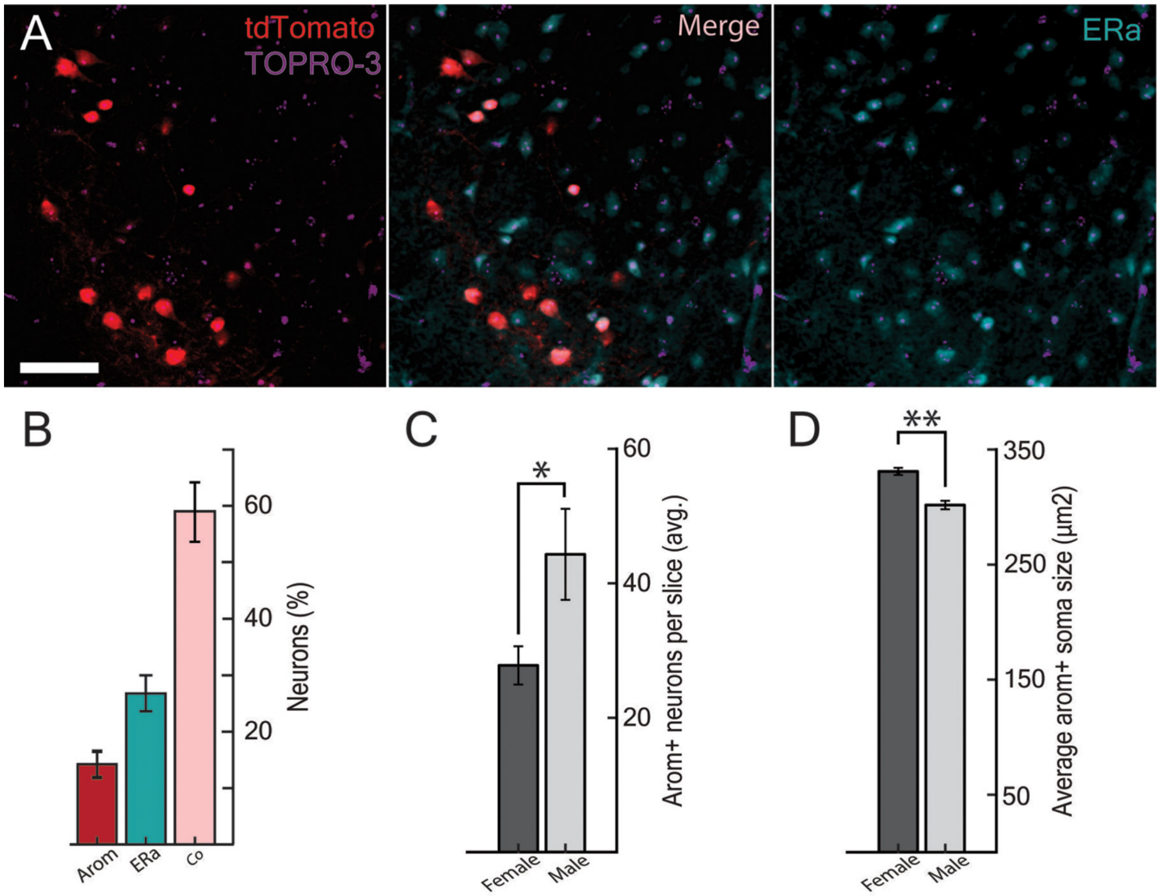

Figure 4.

Arom+→AOB neurons express ERα and are sexually dimorphic. A, ERα (cyan) was labeled through fluorescent immunohistochemistry and colocalized with a subset of arom+ neurons (red) in the MEAv with TOPRO to identify all nuclei (purple). B, 59.0 ± 2.8 % of neurons that were labeled by either ERα antibodies or tdTomato were co-labeled for both—close to the expected joint probability of approximately 63% based on independent distributions. C, More arom+ neurons are found in the male MEAv than in the female MEAv ($p = 0.039$; two-sample t-test). D, The average cell body was larger in the female MEAv than in the male MEAv ($p = 0.0042$, two-way nested ANOVA).

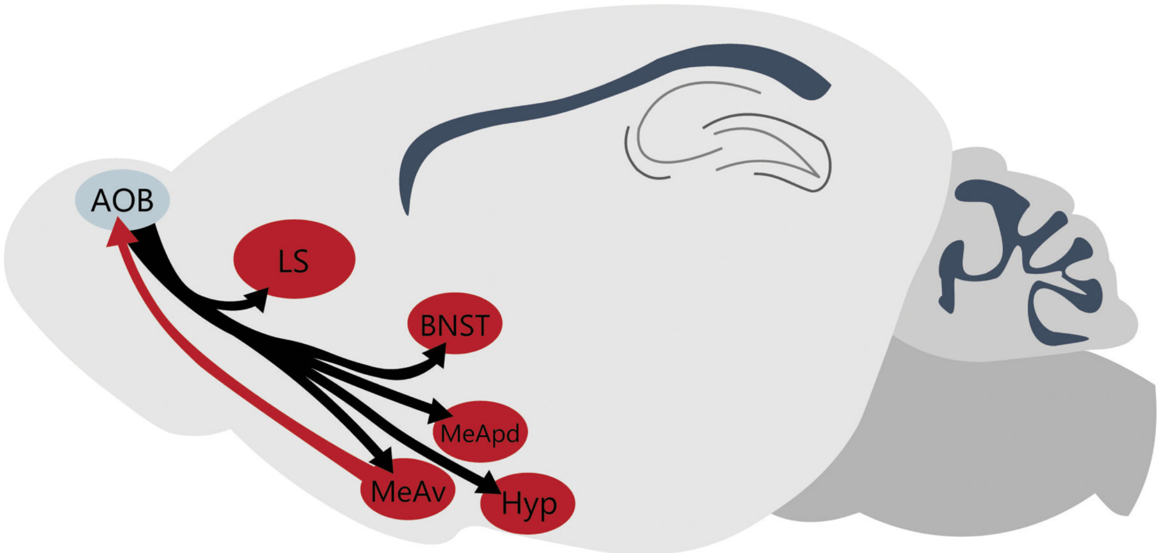

Figure 5.

Circuit anatomy of the AOB including efferent and afferent arom+ targets. The AOB projects to numerous areas with arom+ populations of neurons (black arrows) but only one population of arom+ neurons in the MEAv (red) projects back to the AOB.